JPEDAV (2005) 26:209-214
DOI: 10.1361/15477030523706
1547-7037/$19.00 ©ASM International

The Pr-Rich Portion of the Ni-Pr System

M. Huang, D. Wu, K.W. Dennis, J.W. Anderegg, R.W. McCallum, and T.A. Lograsso

(Submitted September 15, 2004; in revised form March 29, 2005)

The Ni-Pr phase diagram on the Pr-rich side was revised using differential thermal analysis, differential scanning calorimetry, and scanning electron microscopy. The existence of four stoichiometric compounds, Ni_2Pr, NiPr, Ni_3Pr_7, and $NiPr_3$, was confirmed; however, the melting temperatures of 766 °C (NiPr), 566 °C (Ni_3Pr_7), and 562 °C ($NiPr_3$) are considerably different from the previously reported values. The same was true for the four eutectic reactions, which were determined to be as follows: liquid (L) (45 ± 1 at.% Pr) ↔ Ni_2Pr + NiPr at a mean temperature of 732 ± 5 °C; L (65 ± 1 at.% Pr) ↔ NiPr + Ni_3Pr_7 at a mean temperature of 550 ± 2 °C; L (72 ± 2 at.% Pr) ↔ Ni_3Pr_7 + $NiPr_3$ at a mean temperature of 557 ± 2 °C; and L (77 ± 1 at.% Pr) ↔ $NiPr_3$ + Pr.

1. Introduction

The results of an investigation[1] of the magnetic properties of some Ni-Pr-Si alloys were of sufficient import to warrant an investigation of the phase diagram equilibria in the Ni-Pr-Si ternary system. Such phase equilibria data could be used to guide future magnetic measurements toward compositional changes that would produce desirable magnetic changes. To accomplish this goal, it was decided to start with investigations of the phase equilibria in the limiting binary systems. Due to the availability of high-purity Pr at this laboratory, it was decided that the initial study should be on one of the binary Pr boundaries, and the Ni-Pr boundary was chosen. A literature search showed that Pan and Nash[2] had evaluated the phase relationships in the Ni-Pr system with all information that was available prior to 1989. The data included two determinations of the Ni-Pr phase diagram: one by Vogel and Fülling[3]; and the other by Pan and Cheng.[4] In both investigations, the proposed diagram was produced primarily from data generated by a combination of differential thermal analysis (DTA) and x-ray diffraction (XRD).

The Vogel-Fülling[3] diagram was based on data from only nine alloys with Pr purity of 98 to 99 mass%. Four intermediate phases were established with the possibility of two more. The Pan-Cheng[4] diagram was based upon a more extensive study with Pr purity being somewhat better than 99.9 mass%. Their diagram was of the same general form as the Vogel-Fülling[3] diagram, but now with seven rather than four to six intermediate phases, and with corresponding melting temperatures and invariant reaction temperatures of the two investigations agreeing only in the most Ni-rich region of the system. In their evaluation of Ni-Pr data, Pan and Nash[2] preferred the Pan-Cheng[4] diagram.

The current study began with an attempt to verify the Pan-Cheng[4] diagram before moving on to the Ni-Pr-Si ternary system. This was done with DTA measurements on five alloys at differing compositions across the system. The results were compatible with the Pan-Cheng[4] diagram to the extent that the diagram contains seven intermediate phases, five eutectic reactions, and four peritectic reactions. Indeed, in the Ni-rich region of the diagram even the melting temperature and the temperatures of the eutectic and peritectic were in good accord with the Pan-Cheng[4] values, but as the mole fraction of Pr increased the new measurements yielded values for the invariant temperatures that were consistently higher than the Pan-Cheng[4] values. The degree of difference tended to increase with increasing Pr content, with some values being as much as 30 to 90 °C higher. On the basis of these preliminary results, a more extensive investigation was undertaken for the region $0.3 < X_{Pr} < 1$, with X_{Pr} being the mole fraction of Pr.

M. Huang, D. Wu, K.W. Dennis, J.W. Anderegg, R.W. McCallum, and **T.A. Lograsso,** Materials and Engineering Physics Program, Ames Laboratory, Iowa State University, Ames, IA 50011-3020. Contact e-mail: mhuang@ameslab.gov.

2. Experimental Procedures

Alloys were prepared from high-purity elements that were supplied by the Materials Preparation Center at the Ames Laboratory. The major impurities in Ni, as measured by glow discharge mass spectroscopy, are as follows: C, ~247 atomic ppm; O, ~94 atomic ppm; Si, ~60 atomic ppm; Cl, ~45 atomic ppm; and F, ~36 atomic ppm. This indicates Ni purity to be ~99.96 at.%, which transforms to ~99.986 mass%. The impurities in Pr, as measured by the same technique, are as follows: O, ~787 atomic ppm; C, ~268 atomic ppm; H, ~189 atomic ppm; N, ~200 atomic ppm; Gd, ~13 atomic ppm; Si, ~428 atomic ppm; and Nd, ~28 atomic ppm. The analytical data indicate a Pr purity of 99.81 at.%, which converts to 99.98 mass%. These analyses indicate an Ni purity that was quite comparable to that used by Pan and Cheng,[4]but the Pr purity is almost an order of magnitude more pure. All alloys were formed by arc-melting appropriate amounts of the constituent elements. Mass losses during melting were <0.5%. Part of each ingot was cut and wrapped with tantalum (Ta) foil, sealed in quartz tubes filled with 99.998% Ar, homogenized in a furnace at 500 °C for two weeks, and then it was furnace-cooled.

The microstructures of the as-cast and annealed samples were investigated by optical microscopy or scanning electron microscopy (SEM). The quantitative analysis of indi-

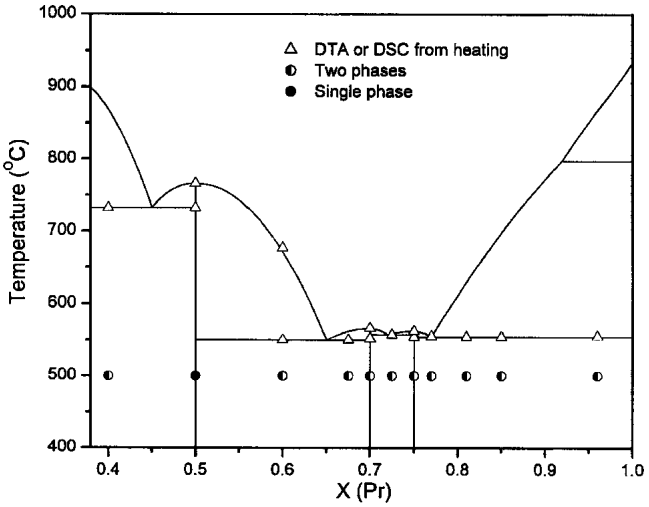

Fig. 1 Pr-rich part of the Ni-Pr phase diagram. The nature of the as-cast microstructure (single or two phase) is indicated.

vidual phases was done by energy-dispersive spectroscopy (EDS) on a JEOL 7830F Auger Microprobe (JEOL, Japan). An analytical uncertainty of no greater than ±1% was obtained by the removal of the oxide layer on the sample surface by ion sputtering and by using single crystals of Ni-Pr-Si ternary alloys as standards. The DTA investigations were carried out in a Perkin Elmer DTA 7 (Perkin Elmer, Wellsley, MA), which can operate to a maximum temperature of 1500 °C. The thermocouples were calibrated at the transition temperature of high-purity K_2SO_4 and at the melting point of Au, and the temperature measurements were accurate to within ±5 °C. For the measurements, samples weighing 20 to 60 mg were cycled at heating and cooling rates of 10 °C/min in Ta crucibles under an Ar atmosphere gettered by Zr at 600 °C with a flow rate of 50 cm^3/min. The Ta crucibles were sealed by arc welding[5] to prevent Pr loss by oxidation or vaporization. Congruent melting temperatures for the stoichiometric compounds Ni_3Pr_7 and $NiPr_3$ could not be resolved from the DTA since they were very close to the invariant temperatures. Therefore, some of the alloys were analyzed in a differential scanning calorimeter (DSC). The thermocouples used in the DSC were calibrated against the melting points of pure In and Al, and the accuracy of the temperature was estimated to be within ±2 °C. DSC measurements for the alloys wrapped with Ta foils were carried out in copper (Cu) pans, which had been crimp-sealed in an Ar glove box. The measurements were conducted at temperatures between room temperature and 700 °C.

3. Results and Discussion

The Pr-rich portion of the Ni-Pr phase diagram resulting from this study is shown in Fig. 1. The existence of compounds NiPr, Ni_3Pr_7, and $NiPr_3$, and the four eutectic reactions were confirmed by EDS and XRD. However, the invariant temperatures are 30 to 90 °C higher than those found in previous studies,[3,4] as listed in Table 1.

Table 1 Invariant reactions in the Pr-rich part of the Ni-Pr system

Reaction	Temperature, °C (at.% Pr in liquid)
Liquid ↔ Ni_2Pr + NiPr	732 (45 ± 1)(a), 680 (~47)(b), 705 (47)(c)
Liquid ↔ NiPr	766(a), 730(b,c)
Liquid ↔ NiPr + Ni_3Pr_7	550(a) (65 ± 1), 510 (~67.5)(b)
Liquid ↔ Ni_3Pr_7	566(a), 535(b)
Liquid ↔ Ni_3Pr_7 + $NiPr_3$	557 (72 ± 1)(a), 490 (~73)(b)
Liquid ↔ $NiPr_3$	562(a), 525(b), 530(c)
Liquid ↔ $NiPr_3$ + Pr	554 (77 ± 1)(a), 460 (~80)(b), 480 (85)(c)

Note: ±SE
(a) This work; (b) Refs 2 and 4; (c) Ref 3

The difference in invariant temperatures found in this study and in the previous study by Vogel and Fülling[3] is possibly due to the experimental methods that were used. While some of the discrepancies can be attributed to the higher purity of the Pr metal used in this study, most of the difference is believed to be related to the high propensity for liquid undercooling in this alloy system. In the current study, invariant temperatures were determined from the onset temperatures of peaks during heating in the DTA or DSC measurements. However, the temperatures determined by Vogel and Fülling[3] were from cooling curves, which are usually lower than those on heating due to undercooling, especially on the Pr-rich side. For example, the onset temperature on heating is about 30 °C higher than that on cooling, as shown in the DSC trace for Ni-85 at.% Pr with a heating/cooling rate of 10 °C/min. The undercooling would be even larger than 30 °C with a cooling rate of 60 °C/min, as used by Vogel and Fülling,[3] which explains the difference of 50 and 74 °C between the current study and that of Vogel and Fülling[3] for the two eutectic reactions on the Pr-rich side. Given the propensity for a large degree of undercooling of the Pr-rich alloys, the as-cast microstructures in this region will not reflect equilibrium solidification structures. In particular, stoichiometric $NiPr_3$ and Ni_3Pr_7 alloys were found to have two phases in the as-cast state, as indicated in Fig. 1. Only following annealing did the structures reflect single-phase stoichiometric compounds.

Figure 2 is a SEM micrograph (taken by backscattered electron [BSE] imaging) of an as-cast Ni-40at.%Pr alloy, which shows primary Ni_2Pr plus Ni_2Pr and NiPr eutectic compositions. The light phase is NiPr, and the dark phase is Ni_2Pr. The eutectic composition was determined by EDS as 45 at.% Pr (66.3 wt.% Pr). The eutectic reaction temperature for L ↔ Ni_2Pr + NiPr at 732 ± 5 °C (±SE) was determined by DTA, as shown in Fig. 3.

The congruent melting temperature of NiPr was determined by DTA at 766 ± 5 °C, as shown in Fig. 4.

Figure 5 shows a BSE micrograph of an as-cast Ni-60at.%Pr alloy with a characteristic eutectic structure corresponding to liquid (L) ↔ NiPr + Ni_3Pr_7. The composition of the eutectic reaction was determined as 65 ± 1 at.% Pr (81.7 wt.% Pr). The eutectic temperature was determined by DTA and DSC to be 550 ± 2 °C, as shown in Fig. 6.

Figure 7 shows a BSE micrograph of as-cast alloy $NiPr_3$. A primary $NiPr_3$ phase surrounded by the Ni_3Pr_7 and $NiPr_3$

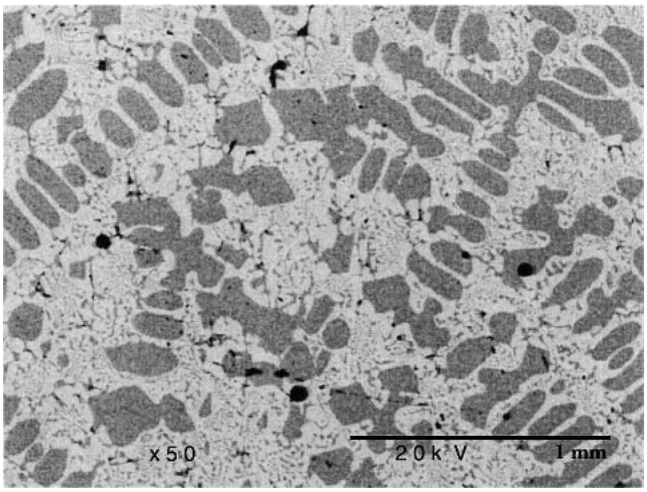

Fig. 2 BSE micrograph of an as-cast Ni-40at.%Pr alloy showing primary Ni_2Pr (gray) surrounded by the Ni_2Pr + NiPr (light) eutectic composition

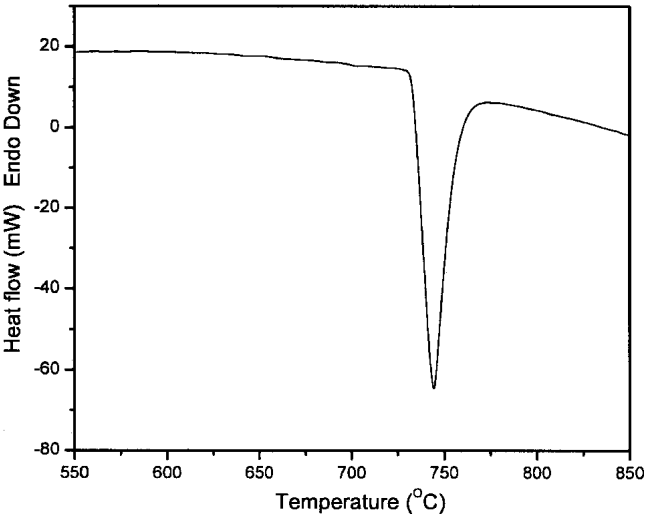

Fig. 3 DTA result of an as-cast Ni-40at.%Pr alloy showing the eutectic reaction of L ↔ Ni_2Pr + NiPr at a mean temperature of 732 ± 5 °C

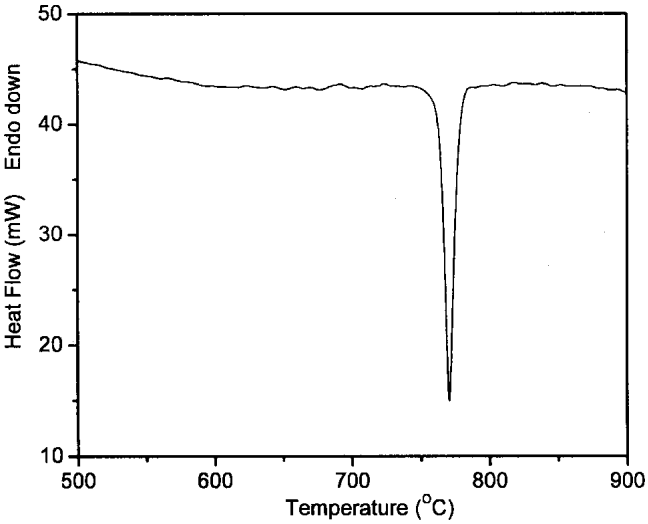

Fig. 4 DTA trace of annealed NiPr alloy

Fig. 5 BSE micrograph of an as-cast Ni-60at.%Pr sample showing primary NiPr surrounded by a NiPr + Ni_3Pr_7 eutectic composition

eutectic compositions was observed. The unexpected presence of primary $NiPr_3$ likely resulted from the high degree of undercooling, leading to metastable solidification conditions resembling an off-eutectic phase distribution rather than single-phase solidification. The composition of the eutectic reaction L ↔ Ni_3Pr_7 + $NiPr_3$ was determined at 72 ± 1 at.% Pr (86.1 wt.% Pr). A eutectic temperature of 557 ± 2 °C was determined by DSC, as shown in Fig. 8.

Figure 9 shows a BSE micrograph of an as-cast Ni-85at.%Pr alloy, and a microstructure of primary Pr dendrites surrounded by a eutectic structure was found. EDS results showed the eutectic reaction L ↔ $NiPr_3$ + Pr at 77 ± 1 at.% Pr (88.9 wt.% Pr). The eutectic temperature of 554 ± 2 °C was determined using a DSC, as shown in Fig. 10.

The major disagreement between the present work and that of Vogel and Fülling[3] and Pan and Cheng[4] concerns the reaction temperatures. The temperature of the eutectic reaction L ↔ NiPr + Ni_2Pr was reported as 705, 680, and 732 ± 5 °C, respectively, by Vogel and Fülling,[3]Pan and Cheng,[4] and this investigation. The current measurements indicate the congruent melting point of NiPr to be 766 ± 5 °C, which is 36 °C higher than the value of 730 °C reported by both of the earlier investigations. For three eutectic reactions, L ↔ NiPr + Ni_3Pr_7, L ↔ Ni_3Pr_7 + $NiPr_3$, and L ↔ $NiPr_3$ + Pr, respective values of 510, 490, and 460 °C were reported by Pan and Cheng,[4] while the values of 550 ± 2, 557 ± 2, 554 ± 2 °C were found in the current study by DSC

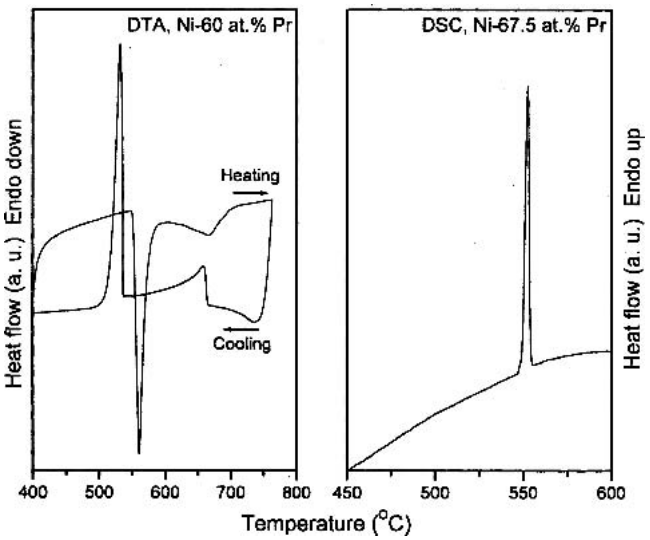

Fig. 6 DTA and DSC results of the as-cast Ni-60at.%Pr and Ni-67.5at.%Pr alloys showing the eutectic reaction L ↔ NiPr + Ni_3Pr_7 at a mean temperature of 550 ± 2 °C

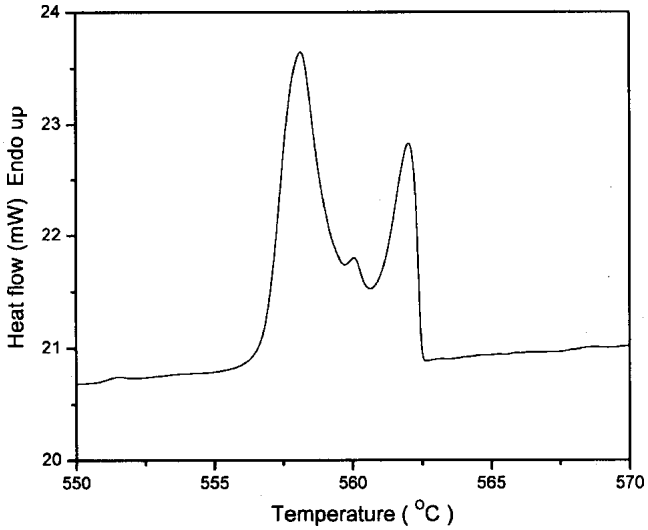

Fig. 8 DSC trace of an $NiPr_3$ alloy at a heating rate of 1 °C/min. The first peak is associated with the eutectic reaction, the second tiny peak is due to the dissolving of the $NiPr_3$ into the liquid, and the third peak is associated with the melting of $NiPr_3$ alloy.

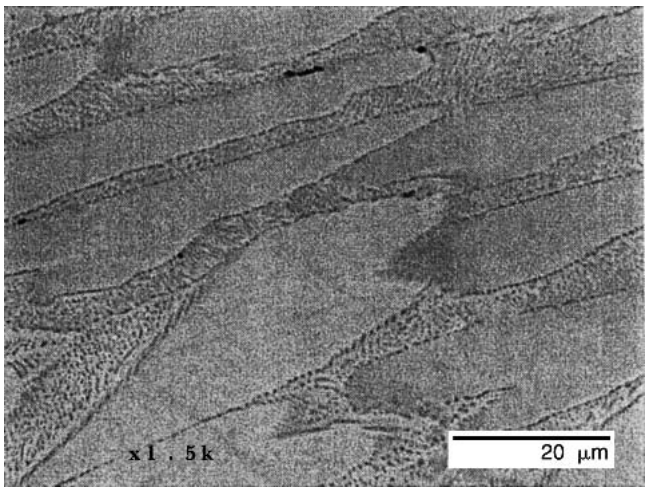

Fig. 7 BSE micrograph of an as-cast $NiPr_3$ alloy showing the primary $NiPr_3$ phase surrounded by the Ni_3Pr_7 + $NiPr_3$ eutectic composition

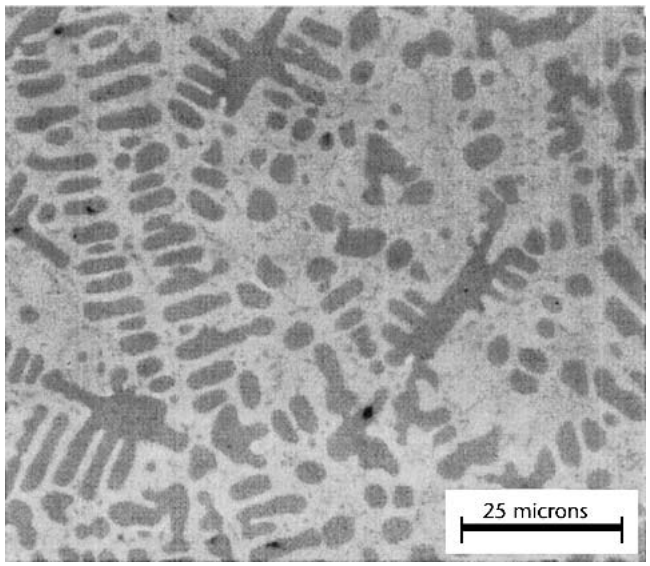

Fig. 9 An optical micrograph of an as-cast Ni-85at.%Pr sample showing a primary Pr and the $NiPr_3$ and Pr eutectic structure

measurements. Due to the limited number of samples used by Vogel and Fulling,[3] they did not find the phase $NiPr_3Pr_7$, so for the region between NiPr and Pr they reported a temperature of 500 °C for what they believed was the eutectic reaction L ↔ NiPr + $NiPr_3$, and a temperature of 480 °C for the eutectic reaction L ↔ $NiPr_3$ + Pr, with both values being well below the currently measured values for this composition region.

The determination of the congruent melting points of the compounds Ni_3Pr_7 (566 ± 2 °C) and $NiPr_3$ (562 ± 2 °C) is challenging. Due to the small difference in composition between the two phases, very small changes in stoichiometry result in large amounts of the second phase, leading to the observation of more than one thermal event. Second, the large degree of undercooling in Pr-rich alloys leads to non-equilibrium as-cast structures, which in turn leads to misleading melting behavior. In addition, the melting temperatures could not be resolved from the DTA due to their close proximity to the invariant temperature (557 °C). DSC measurements with a heating rate of 10 °C /min were then carried out on the annealed compounds Ni_3Pr_7 and $NiPr_3$ to determine the melting points. Despite the higher resolution of the DSC measurements, it was found that the thermal signal associated with congruent melting overlapped with the eutectic reaction, resulting in the peak position of the combined thermal event to shift with heating/cooling cycles due to the oxidation of Pr during heating, despite the fact

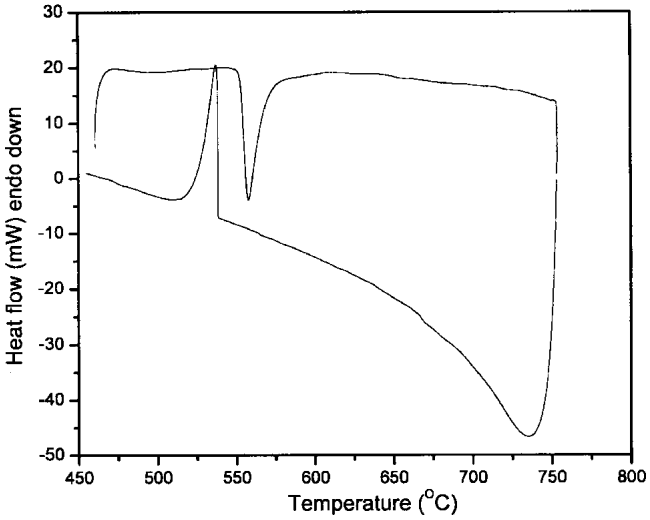

Fig. 10 DTA result of an as-cast Ni-85at.%Pr alloy

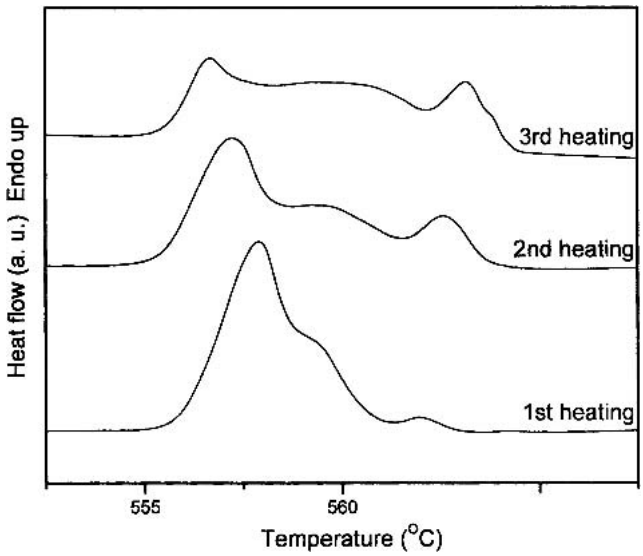

Fig. 11 DSC results of as-cast Ni-77at.%Pr alloy. The first peak is associated with the eutectic reaction, the hump is associated the dissolving of the $NiPr_3$ into the liquid, and the third peak is associated with the melting of $NiPr_3$. It can be seen that the peak for the eutectic reaction decreased and that for the melting of $NiPr_3$ increased due to oxidation of Pr with cycles.

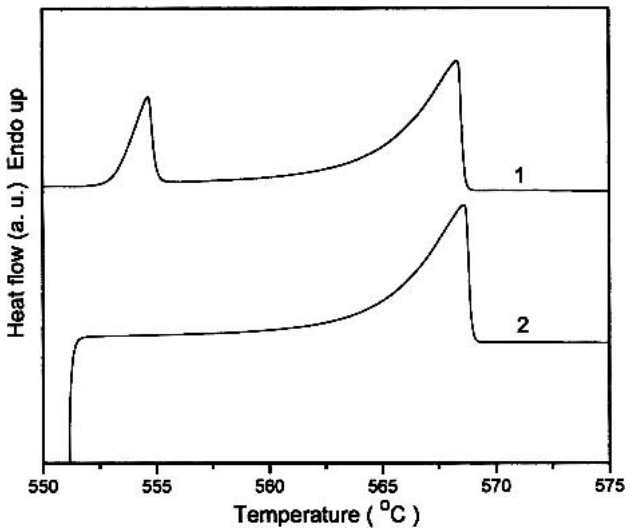

Fig. 12 DSC results of Ni_3Pr_7 alloy. The first peak in curve 1 is associated with the eutectic reaction L ↔ NiPr + Ni_3Pr_7, and the second peak is associated with the melting of Ni_3Pr_7. Curve 2 was obtained by heating the sample to 560 °C and holding for 10 min, then cooling to 550 °C, and then reheating to 580 °C.

that the samples were wrapped in Ta foil and crimp-sealed in Cu pans in an Ar glovebox. For example, during the heating of the $NiPr_3$ alloys in the DSC, three thermal events occurring very close in temperature (557, 562, and 566 °C) were found, overlapping each other, in the first heating. After several heating cycles, the peaks shifted, which made it difficult to determine which reactions corresponded to which peaks.

To obtain repeatable results, the composition for $NiPr_3$ alloys should always be Pr-rich (slightly >75 at.% Pr), so that only two peaks (one for the eutectic phase and one for the $NiPr_3$ liquidus) can be observed during the measurements. In this case, an alloy of Ni-77at.%Pr was used to determine the congruent melting point of $NiPr_3$, as shown in Fig. 11. During the first heating, the biggest peak is associated with the eutectic reaction between Pr and $NiPr_3$ at 554 °C, the second hump is due to the dissolution of $NiPr_3$ into liquid, and the third tiny peak is associated with the melting of remaining $NiPr_3$ (i.e., the liquidus temperature). Due to the oxidation of Pr during subsequent cycles, the overall composition is depleted in Pr and the fraction of $NiPr_3$ is increased, thereby enhancing the peak of melting, as shown in the second and third heating, and separating the two thermal events, which correspond to the eutectic reaction and melting from each other.

For Ni_3Pr_7, repeated cycling was not necessary if the alloy composition was Ni-rich (i.e., slightly >30 at.% Ni). In this case, the two thermal signals can be well resolved because the difference between the melting temperature (566 °C) and eutectic temperatures is larger on the Ni-rich side (550 °C) than the Pr-rich side (557 °C). During measurements, the annealed stoichiometric Ni_3Pr_7 was used as a starting material, and after several cycles the composition shifted to the Ni-rich side, and only two peaks at 550 and 566 °C were found in curve 1, as shown in Fig. 12. These two peaks corresponded to the eutectic reaction between Ni_3Pr_7 and NiPr and the congruent melting point of Ni_3Pr_7, respectively. The only peak in curve 2 is the congruent melting point of Ni_3Pr_7. To obtain this curve, the sample was first heated through the eutectic temperature and held at a temperature below the congruent melting point of Ni_3Pr_7, such that the eutectic liquid equilibrated with solid Ni_3Pr_7, then cooled to a temperature just above the eutectic invariant freezing, and heated again through the congruent melting temperature.

The determination of liquidus curves is problematic for an experimental phase diagram study because multiple

samples are required to get adequate results, especially within small compositional ranges like those associated with $NiPr_3$ and Ni_3Pr_7. Further, it is often impossible to gather accurate temperature measurements from DTA or DSC traces because there are insufficient thermal signatures for the dissolution of the trace remaining solid. Thermodynamic modeling, on the other hand, is a good tool for phase diagram study if some experimental data are available. In the current study, the liquidus curves shown in Fig. 1 were predicted by thermodynamic modeling carried out using WinPhad (Computherm LLC, Madison, WI), a computer program developed by Y. Austin Chang and coworkers for the calculation of a phase diagram. During modeling, the phase equilibria and available thermodynamic data for the Ni-Pr system were optimized to produce thermodynamic functions to describe the Gibbs energies of individual phases. The liquid phase was treated as a subregular solution. The intermetallic phases were regarded as line compounds. Details of the optimization process with the resultant parameters have been discussed by Huang and Lograsso.[6]

4. Conclusions

The Ni-Pr alloy phase diagram on the Pr-rich side was reinvestigated by DTA, DSC, SEM, and thermodynamic modeling. The melting temperatures for three compounds have been adjusted to 766 °C for NiPr, 566 °C for Ni_3Pr_7, and 562 °C for $NiPr_3$. The four eutectic reactions were revised as follows: L $\leftrightarrow$ Ni_2Pr + NiPr at 45 ± 1 at.% Pr (66.3 wt.% Pr) at a temperature of 732 ± 5 °C; L $\leftrightarrow$ NiPr + Ni_3Pr_7 at 65 ± 1 at.% Pr (81.7 wt.% Pr) at a temperature of 550 ± 2 °C; L $\leftrightarrow$ Ni_3Pr_7 + $NiPr_3$ at 72 ± 1 at.% Pr (86.1 wt.% Pr) at a temperature of 557 ± 2 °C; and L $\leftrightarrow$ $NiPr_3$ + Pr at 77 ± 1 at.% Pr (88.9 wt.% Pr) at a temperature of 554 ± 2 °C.

Acknowledgments

The preliminary samples that motivated this work were provided by A.O. Pecharsky. This work was supported by the U.S. Department of Energy, Office of Basic Energy Science, Materials Science Division. The research was performed at Ames Laboratory. Ames Laboratory is operated for the U.S. Department of Energy by Iowa State University under Contract No. W-7405-ENG-82.

References

1. A.O. Pecharsky, Y. Mozharivskyj, K.W. Dennis, K.A. Gschneidner, Jr., R.W. McCallum, G.J. Miller, and V.K. Pecharsky, Preparation, Crystal Structure, Heat Capacity, Magnetism, and the Magnetocaloric Effect of Pr5Ni1.9Si3 and PrNi, *Phys. Rev. B: Condens. Matter,* Vol 68, 2003, p 134452/1-134452/8
2. Y.Y. Pan and P. Nash, The Ni-Pr (Nickel-Praesodymium) System, *Bull. Alloy Phase Diagrams,* Vol 10, 1989, p 253-257, 305-306
3. R. Vogel and W. Fülling, The Systems of Cerium-Nickel, Lanthanum-Nickel, Praseodymium-Nickel and Cerium-Cobalt, *Metallforschung,* Vol 2, 1947, p 97-103
4. Y.Y. Pan and C.S. Cheng, The Phase Equilibria in Ni-Pr System, presented at Chinese National Symposium on Phase Diagrams (Kunming, Peoples Republic of China), September 1984 (in Chinese)
5. Y. Jansen, Ames Laboratory, 2004, personal communication
6. M. Huang and T.A. Lograsso, Experimental Investigation and Thermodynamic Modeling of the Ni-Pr System, *J. Alloys Compd.*, Vol 395, 2005, p 75-79, available at: doi:10.1016/j.jallcom.2004.11.039